

# Spin-spin correlations of magnetic impurities in graphene

A. D. Güçlü and Nejat Bulut

*Department of Physics, Izmir Institute of Technology, IZTECH, TR35430, Izmir, Turkey*

(Dated: October 1, 2018)

We study the interaction between two magnetic adatom impurities in graphene using the Anderson model. The two-impurity Anderson Hamiltonian is solved numerically by using the quantum Monte Carlo technique. We find that the inter-impurity spin susceptibility is strongly enhanced at low temperatures, significantly diverging from the well-known Ruderman-Kittel-Kasuya-Yoshida (RKKY) result which decays as  $R^{-3}$ .

Graphene[1–4], a two-dimensional honeycomb lattice of carbon atoms, shows promise as a material for nano-electronics due to high electronic and thermal conductivity. Moreover, graphene structures engineered at the nanoscale are shown to give rise to unique magnetic properties due to the formation of finite magnetic moments at the edges[5–14], which could be important for nano-electronic and spintronic device applications. Another way of probing magnetism in graphene is through the exchange interaction between impurity atoms mediated by the host electrons, known as RKKY interaction[15–20]. Understanding the effective interaction between impurity atoms in graphene is also important from fundamental physics point of view since the excitations on a honeycomb lattice are massless Dirac fermions, giving rise to a behavior different from semiconductor or metal host structures[15–20].

The RKKY interaction in graphene exhibits unique features different from other two-dimensional systems. In Ref.21, it was predicted that RKKY interaction should decay as  $R^{-3}$  in contrast with  $R^{-2}$  behaviour found in a two-dimensional electron gas[22], where  $R$  is the distance between the two impurities. This was later confirmed in Ref.17 where other important features of RKKY interaction in graphene were clarified as well. In particular, a general proof regarding the sign of the RKKY interaction in a half-filled bipartite lattice was given: interaction between moments sitting on the same (opposite) sublattice(s) is ferromagnetic (antiferromagnetic). We note that the biparticity of the graphene lattice is also at the hearth of Lieb’s theorem on magnetism[23] which gives rise to edge magnetism in graphene nanostructures[12–14]. In Ref.17, it was also shown that the RKKY interaction is subject to an oscillatory term of the type  $1 + \cos(2\Delta\mathbf{k} \cdot \mathbf{R})$  ( $2k_F$  oscillations), where  $\Delta\mathbf{k}$  is the reciprocal lattice vector connecting two Dirac points in the Brillouin zone. All these features were confirmed by others[18–20] using different approximation schemes. It should be noted that impurities do not have to sit on top of a particular atom, but can bond with several neighboring atoms. In fact, mechanical and electronic properties of various adatoms on graphene were previously investigated [24–31]. GGA+U calculations[28] show that the particular bonding configuration may de-

pend on the value of the on-site interaction parameter  $U$ . However, according to RKKY analysis [17], the interaction between plaquette-type impurities (where the impurity atom bonds with the six Carbon atoms of a hexagon in the honeycomb lattice) is much weaker and decays rapidly as  $R^{-4}$ . This is also consistent with our QMC results (not shown). Therefore, in the following we will focus on the interaction between impurities with on-top configuration.

In this work, we use the Hirsch-Fye quantum Monte Carlo (QMC) method[32] to calculate the magnetic susceptibilities of the two-impurity Anderson model. We find that, although the biparticity theorem of Ref.17 and the  $2k_F$  oscillation behaviour are not affected by electron-electron interactions, the long range behaviour of the effective RKKY interaction is strongly enhanced, becoming several orders of magnitude larger at longer distances.

The two-impurity Anderson model for a graphene host is given by

$$H = \sum_{\mathbf{k}\alpha\sigma} \epsilon_{\mathbf{k}} c_{\mathbf{k}\alpha\sigma}^\dagger c_{\mathbf{k}\alpha\sigma} + E_d \sum_{i\sigma} d_{i\sigma}^\dagger d_{i\sigma} + \sum_{\mathbf{k}\alpha i\sigma} \left( V_{\mathbf{k}\alpha i} c_{\mathbf{k}\alpha\sigma}^\dagger d_{i\sigma} + \text{h.c.} \right) + U \sum_i n_{i\uparrow} n_{i\downarrow} \quad (1)$$

where  $c_{\mathbf{k}\alpha\sigma}^\dagger$  creates a host electron with wavevector  $\mathbf{k}$  and spin  $\sigma$  in the valence  $\alpha = v$  or conduction  $\alpha = c$  band,  $d_{i\sigma}^\dagger$  creates an electron at the impurity site  $i$ , and  $n_{i\sigma} = d_{i\sigma}^\dagger d_{i\sigma}$ . In addition,  $U$  is the onsite Coulomb repulsion and  $E_d$  is the impurity energy level. The electronic spectrum of the graphene host  $\epsilon_{\mathbf{k}}$  and the hybridization matrix elements  $V_{\mathbf{k}\alpha i}$  are calculated analytically in terms of graphene structure factor  $f(\mathbf{k})$  in the nearest neighbour approximation with hopping parameter  $t$ . The impurity-carbon atom hybridization parameter is denoted by  $V$ . The calculations are performed within the symmetric Anderson model where  $E_d = -U/2$ , as a function of inverse temperature  $\beta = 1/T$  and the distance between the two impurities  $R$ .

The numerical results presented here were obtained using the Hirsch-Fye quantum Monte Carlo technique which allows us to compute the Matsubara single-particle Green’s functions for impurity sites  $i$  and  $j$ ,

$$G_{ij}^\sigma(\tau) = -\langle T_\tau d_{i\sigma}(\tau) d_{j\sigma}^\dagger(0) \rangle, \quad (2)$$

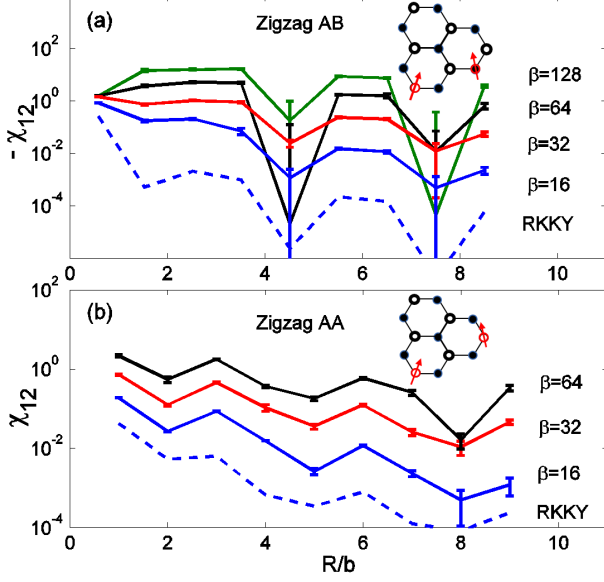


FIG. 1: The static magnetic susceptibility between two magnetic adatom impurities along the zigzag direction as a function of distance for (a) the AB configuration (impurities on opposite sublattices, shown in the inset) and (b) the AA configuration (impurities on the same sublattice, shown in the inset), obtained by QMC calculations at different inverse temperatures  $\beta$ . The dashed lines are the RKKY results from Ref.19. The magnetic coupling obtained by the QMC shows the same ferromagnetic and antiferromagnetic behaviour, and the  $2k_F$  oscillations as in the RKKY results. However, at low temperatures, the effective magnetic coupling becomes much stronger and the QMC results diverge from the RKKY's  $R^{-3}$  decay.

where  $T_\tau$  is the Matsubara time-ordering operator and  $d_{i\sigma}(\tau) = e^{H\tau} d_{i\sigma} e^{-H\tau}$ . In addition, we calculate the zero-frequency inter-impurity magnetic susceptibility using:

$$\chi_{12}(\omega = 0) = \int_0^\beta d\tau \langle M_1^z(\tau) M_2^z(0) \rangle, \quad (3)$$

where  $M_i^z = n_{id\uparrow} - n_{id\downarrow}$ . Local magnetic moment of impurity adatoms on graphene were studied in Ref.33. Here we concentrate on the impurity-impurity magnetic correlations.

In Fig.1, we consider the case where the two impurities are located along the zigzag direction of the honeycomb lattice, sitting on different (zigzag AB, Fig.1a) and same (zigzag AA, Fig.1b) sublattices. The static magnetic susceptibilities  $\chi_{12}$  given in Eq.3 are calculated as a function of the distance between the impurities  $R$  (in units of the second nearest neighbour distance  $b$ ) at different inverse temperatures  $\beta$  expressed in units of  $t^{-1}$ . We take  $V = t$  and  $U = 0.8t$  (see Fig.2 for larger values of  $U$ ). Here, the results are also compared to the analytical RKKY results[19] denoted by the dashed lines. For the AB configuration, the RKKY model yields to an antiferromag-

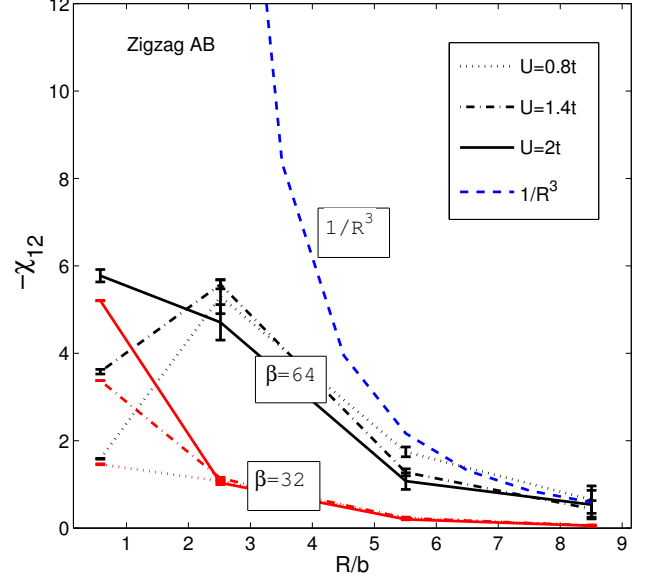


FIG. 2: The static magnetic susceptibility between two magnetic adatom impurities along the zigzag direction as a function of distance for the AB configuration obtained using QMC method, at different inverse temperatures  $\beta$  and different  $U$ . The dashed lines show the  $R^{-3}$  decay predicted by the RKKY model. Even at the highest  $U$  value QMC calculations yield much longer-ranged effective magnetic coupling between the adatoms.

netic coupling between the two impurities as seen from the sign of  $\chi_{ij}$ , and Fermi oscillations with minima at every  $(2 + 3n)$ th B-atom along the zigzag AB direction. For the AA configuration, the coupling is ferromagnetic and the oscillations have maximum at every  $(3 + 3n)$ th A-atom. For both cases, as already mentioned, the oscillations decay as  $R^{-3}$ . All these behaviours agree well with the Anderson model (QMC) results especially at higher temperatures. However, the results are very sensitive to the temperature. As the temperature is lowered, significant deviations from RKKY results occur. The overall magnitude of the static susceptibility increases by several orders especially at larger  $R$  values, the decay of RKKY becomes much slower, and the Fermi oscillations become less prominent. Strikingly, at  $\beta = 128t^{-1}$  which corresponds to  $T = 272$  K for  $t = 3$  eV, there is no decay in the range of  $R$  studied here.

In Fig.2, we investigate the effect of  $U$  on the static susceptibility. The susceptibilities are calculated at  $\beta = 32t^{-1}$  and  $\beta = 64t^{-1}$  for the zigzag AB case (similar to Fig.1a but in linear scale instead of logarithmic). Calculations are repeated for  $U = 0.8t$ ,  $1.4t$ , and  $U = 2t$ , corresponding to 2.4 eV, 4.2 eV, and 6 eV, respectively. Although the exact value for  $U$  is not known for 3d transition metal adatoms in graphene, its effective value is estimated to be in the range of 2-4 eV [27–30]. As the

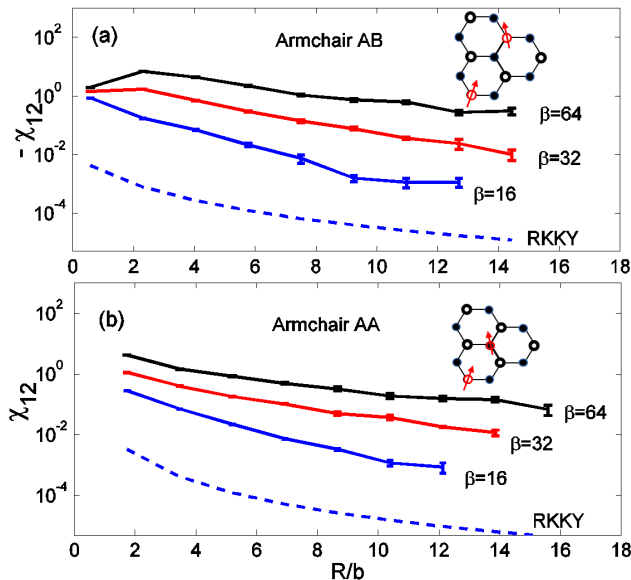


FIG. 3: The static magnetic susceptibility between two magnetic adatom impurities along the armchair direction as a function of distance for (a) the AB configuration (shown in the inset) and (b) the AA configuration (shown in the inset), obtained by QMC calculations at different inverse temperatures  $\beta$ . The dashed lines are RKKY results from Ref.19. The magnetic coupling from QMC show the same ferromagnetic and antiferromagnetic behaviour. At low temperatures, the effective magnetic coupling becomes much stronger and the QMC results diverge from the RKKY's  $R^{-3}$  decay.

statistical fluctuations increase for larger values of  $U$  in QMC calculations, the analysis is restricted to four different values of  $R$  corresponding to first, third, sixth, and ninth atoms (along the zigzag direction) belonging to the maxima of the RKKY oscillations. Clearly the main effect of increasing  $U$  is to increase the susceptibility for  $R/b < 3$ , i.e. at very short ranges. For  $R/b > 3$ , we do not observe a significant change in  $\chi_{ij}(R)$  within our statistical accuracy. The overall behaviour thus becomes slightly closer in shape to the  $R^{-3}$  decay (dashed curve), but there are still several orders of magnitude of difference between the RKKY and Anderson model results. Thus, the main conclusions of Fig.1 remains unchanged for the values of  $U$  considered here.

We now turn to the armchair configuration. In Fig.3, the results are presented for  $U = 0.8t$  at different values of  $\beta$ , for the AB and AA configurations. Again the antiferromagnetic and ferromagnetic phases for the AB and AA configurations are consistent with the RKKY model. Note that along the armchair direction, the RKKY model does not exhibit Fermi oscillations. This is also consistent with the QMC results at higher temperatures (lower  $\beta$ ) which show no clear structure within our statistical accuracy. As the temperature is lowered, similar to the

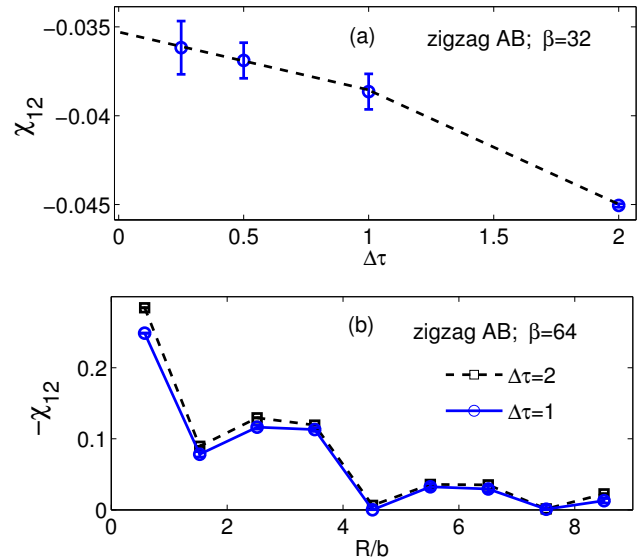


FIG. 4: The static magnetic susceptibility between two magnetic adatom impurities along the zigzag for the AB configuration obtained using QMC method, at different time-step  $\Delta\tau$ , (a) for  $\beta = 32t^{-1}$  and  $R/b \sim 2.5$  (b) as a function of  $R$  for  $\beta = 64t^{-1}$ . These results show that the finite time-step error is under control.

zigzag case, the static susceptibility increases by more than two orders of magnitude at larger distances of the order  $R/b \sim 10$  significantly deviating from the  $R^{-3}$  behaviour.

We note that the long-range behaviour of the impurity-impurity correlations observed in our numerical results for the Anderson model is consistent with the predictions of Lieb's theorem for the Hubbard model in bipartite systems. According to Lieb's theorem[23], if there is an imbalance between the number of A and B sublattice atoms, a finite magnetic moment  $(N_A - N_B)/2$  arises at zero temperature. In our case, each impurity breaks the symmetry between the two sublattices locally. Thus, if the impurities are far from each other, locally a finite magnetic moment must appear at each impurity location. If the two impurities are on same sublattices the magnetic moments must add, or otherwise cancel each other, giving rise to a strong ferromagnetic or antiferromagnetic inter-impurity correlation.

We now discuss the finite time-step error involved in numerical calculations. In the QMC method, the partition function is discretized using  $Z = \text{Tr} \prod^L \exp(-\Delta\tau H)$  where  $\Delta\tau$  is size of the time-step,  $L$  is the number of Monte Carlo time-slices, and  $\beta = L\Delta\tau$ .  $Z$  defined above approaches the exact partition function of the system in the limit of infinite  $L$ , i.e. small  $\Delta\tau$ . In order to check the effect of using finite time-step, Fig.4a shows  $\chi_{ij}(R)$  for the third nearest AB-neighbours along the zigzag di-

rection calculated for  $\beta = 64t^{-1}$  using  $\Delta\tau = 2, 1, 0.5$  and  $0.25$  in units of  $t^{-1}$ . Actual calculations are done for  $\Delta\tau = 1$  in previous figures. The estimated time-step error is within few error bars. We also plotted in Fig.1b the results obtained for  $\beta = 64t^{-1}$  using  $\Delta\tau = 2$  and  $1$ , showing the finite time-step error is under control in our calculations

In conclusion, we studied the interaction between two magnetic adatom impurities in graphene within the Anderson model by using the quantum Monte Carlo technique. Our results yield to the same magnetic phases predicted by RKKY: ferromagnetic for the AA (same sublattice) configuration and antiferromagnetic for the AB (opposite sublattice) configuration. Moreover,  $2k_F$  oscillations similar to those of RKKY exist. However, due to electron-electron interactions, the magnetic coupling between the impurities becomes more than two orders of magnitude stronger than what is predicted by the RKKY model, especially at lower temperatures. In addition, the results significantly diverge from the  $R^{-3}$  decay predicted by RKKY and the effective interaction between the impurities become long-ranged.

*Acknowledgment.* This research was supported by a BIDEP Grant from TÜBİTAK, Turkey, and by a BAGEP grant from Bilim Akademisi - The Science Academy, Turkey.

- 
- [1] P. R. Wallace, Phys. Rev. **71**, 622 (1947).  
 [2] A. H. C. Neto, F. Guinea, N. M. R. Peres, K. S. Novoselov, and A. K. Geim, Rev. of Mod. Phys., **81**, 109 (2009).  
 [3] K. S. Novoselov, A. K. Geim, S. V. Morozov, D. Jiang, Y. Zhang, S. V. Dubonos, I. V. Grigorieva, A. A. Firsov, Science, **306**, 666 (2004).  
 [4] Y. B. Zhang, Y. W. Tan, H. L. Stormer, P. Kim, Nature, **438**, 201 (2005).  
 [5] M. Wimmer, I. Adagideli, S. Berber, D. Tomanek, and K. Richter, Phys. Rev. Lett. **100**, 177207 (2008).  
 [6] O. V. Yazyev, M. I. Katsnelson, Phys. Rev. Lett. **100**, 047209 (2008).  
 [7] L. Yang, M. L. Cohen and S. G. Louie, Phys. Rev. Lett. **101**, 186401 (2008).  
 [8] J. Jung and A. H. MacDonald, Phys. Rev. B **79**, 235433 (2009).  
 [9] F. Munoz-Rojas, J. Fernandez-Rossier, J.J. Palacios, Phys. Rev. Lett. **102**, 136810 (2009).  
 [10] B. Wunsch, T. Stauber, F. Sols, F. Guinea, Phys. Rev. Lett. **101** 036803 (2008).  
 [11] S. Dutta, S. Lakshmi, and S. K. Pati, Phys. Rev. B **77**, 073412 (2008).  
 [12] A. D. Güçlü, P. Potasz, O. Voznyy, M. Korkusinski, P. Hawrylak, Phys. Rev. Lett. **103**, 246805 (2009).  
 [13] P. Potasz, A. D. Güçlü, A. Wojs, and P. Hawrylak, Phys. Rev. B **85**, 075431 (2012).  
 [14] A.D. Güçlü, M. Grabowski, P. Hawrylak, Phys. Rev. B **87**, 035435 (2013).  
 [15] S. R. Power and M. S. Ferreira, Crystals **3**, 49 (2013).  
 [16] L. Brey, H. A. Fertig, and S. Das Sarma Phys. Rev. Lett. **99**, 116802 (2007).  
 [17] Saeed Saremi, Phys. Rev. B **76**, 184430 (2007).  
 [18] Annica M. Black-Schaffer Phys. Rev. B **81**, 205416 (2010).  
 [19] M. Sherafati and S. Satpathy, Phys. Rev. B **83**, 165425 (2011).  
 [20] E. Kogan, Phys. Rev. B **84**, 115119 (2011).  
 [21] B. Wunsch, T. Stauber, F. Sols, and F. Guinea, New J. Phys. **8**, 318 (2006).  
 [22] Baruch Fischer and Michael W. Klein Phys. Rev. B **11**, 2025 (1975).  
 [23] E. H. Lieb, Phys. Rev. Lett. **62**, 1201 (1989).  
 [24] H. Sevincli, M. Topsakal, E. Durgun, and S. Ciraci, Phys. Rev. B **77**, 195434 (2008).  
 [25] Y.G. Zhou, X.T. Zu, F. Gao, H.F. Lv, and H.Y. Xiao, Applied Physics Letters, **95**, 123119 (2009).  
 [26] R. Xiao, D. Fritsch, M. D. Kuzmin, K. Koepnik, H. Eschrig, M. Richter, K. Vietze, and G. Seifert, Phys. Rev. Lett. **103**, 187201 (2009).  
 [27] D. Jacob and G. Kotliar, Phys. Rev. B **82**, 085423 (2010).  
 [28] T. O. Wehling, A. V. Balatsky, M. I. Katsnelson, A. I. Lichtenstein, and A. Rosch, Phys. Rev. B **81**, 115427 (2010).  
 [29] K. T. Chan, H. Lee, and M. L. Cohen, Phys. Rev. B **83**, 035405 (2011).  
 [30] A. N. Rudenko, F. J. Keil, M. I. Katsnelson, and A. I. Lichtenstein, Phys. Rev. B **86**, 075422 (2012).  
 [31] A. Saffarzadeh and G. Kirzenow, Phys. Rev. B **85**, 245429 (2012).  
 [32] J. E. Hirsch and R. M. Fye Phys. Rev. Lett. **56**, 2521 (1986).  
 [33] F. M. Hu, Tianxing Ma, Hai-Qing Lin, and J. E. Gubernatis, Phys. Rev. B **84**, 075414 (2011).